

# Development of an Affinity-Based Probe to profile endogenous Human Adenosine A<sub>3</sub> Receptor Expression

Bert L. H. Beerkens<sup>[a]</sup>, Inge M. Snijders<sup>[a]</sup>, Joep Snoeck<sup>[a]</sup>, Rongfang Liu<sup>[a]</sup>, Anton T. J. Tool<sup>[b]</sup>, Sylvia E. Le Dévédec<sup>[a]</sup>, Willem Jaspers<sup>[a]</sup>, Taco W. Kuijpers<sup>[b, c]</sup>, Gerard J.P. van Westen<sup>[a]</sup>, Laura H. Heitman<sup>[a, d]</sup>, Adriaan P. IJzerman<sup>[a]</sup>, and Daan van der Es<sup>\*[a]</sup>

---

[a] Division of Drug Discovery and Safety, Leiden Academic Centre for Drug Research, Leiden University, Einsteinweg 55, 2333 CC Leiden, The Netherlands, E-mail: d.van.der.es@lacdr.leidenuniv.nl

[b] Department of Molecular Hematology, Sanquin Research, Plesmalaan 125, 1066 CX Amsterdam, The Netherlands

[c] Department of Pediatric Immunology, Rheumatology and Infectious Diseases, Emma Children's Hospital, Academic Medical Center, University of Amsterdam, Amsterdam, The Netherlands, Meibergdreef 9, 1105 AZ Amsterdam, The Netherlands

[d] Oncode Institute, Einsteinweg 55, 2333 CC, Leiden, The Netherlands

## Abstract

The adenosine A<sub>3</sub> receptor (A<sub>3</sub>AR) is a G protein-coupled receptor (GPCR) that exerts immunomodulatory effects in pathophysiological conditions such as inflammation and cancer. Thus far, studies towards the downstream effects of A<sub>3</sub>AR activation have yielded contradictory results, thereby motivating the need for further investigations. Various chemical and biological tools have been developed for this purpose, ranging from fluorescent ligands to antibodies. Nevertheless, these probes are limited by their reversible mode of binding, relatively large size and often low specificity. Therefore, in this work, we have developed a clickable and covalent affinity-based probe (AfBP) to target the human A<sub>3</sub>AR. Herein, we show validation of the synthesized AfBP in radioligand displacement, SDS-PAGE and confocal microscopy experiments, as well as utilization of the AfBP for the detection of endogenous A<sub>3</sub>AR expression in flow cytometry experiments. Ultimately, this AfBP will aid future studies towards the expression and function of the A<sub>3</sub>AR in pathologies.

## Introduction

Adenosine is a signaling molecule that is the endogenous agonist to four adenosine receptors (ARs): the A<sub>1</sub>, A<sub>2A</sub>, A<sub>2B</sub> and A<sub>3</sub> adenosine receptors (A<sub>1</sub>AR, A<sub>2A</sub>AR, A<sub>2B</sub>AR and A<sub>3</sub>AR) that are members of the larger G protein-coupled receptor (GPCR) family.<sup>[1-3]</sup> Activation of the ARs via binding of adenosine induces a cascade of intracellular signaling pathways, that in turn modulate the cellular response to physiological and pathophysiological conditions, examples being inflammation, autoimmune disorders and cancers.<sup>[4-6]</sup>

The ARs are expressed on diverse cell and tissue types, in which the receptors all exert their own functions.<sup>[1]</sup> In case of the human A<sub>3</sub>AR (hA<sub>3</sub>AR), the receptor has been found expressed on granulocytes: eosinophils, neutrophils and mast cells, among other cell types.<sup>[7-10]</sup> Here, activation of the hA<sub>3</sub>AR leads to various immunomodulatory effects, ranging from degranulation to influencing chemotaxis.<sup>[7-13]</sup> However, multiple contradictory observations have been reported regarding the activation of hA<sub>3</sub>ARs. For example, both inhibition and promotion of chemotaxis have been observed upon addition of a selective hA<sub>3</sub>AR agonist to neutrophils.<sup>[11,13,14]</sup> Next to that, expression of the hA<sub>3</sub>AR is species-dependent, and large differences in hA<sub>3</sub>AR activity have been found between humans and rodents.<sup>[15,16]</sup> Thus, many questions regarding activity and functioning of the hA<sub>3</sub>AR, whether on granulocytes or on other cell types and tissues, remain unanswered.

Most of the aforementioned studies have been carried out using selective ligands, e.g. agonists or antagonists to induce a cellular response as read-out. This has yielded valuable information on a biological level but ignores multiple factors that influence receptor signalling on a molecular level, such as receptor localization, protein-protein interactions (PPIs) and

post-translational modifications (PTMs).<sup>[17]</sup> Traditionally, these aspects would be studied using antibodies. However, antibodies for GPCRs are hindered in their selectivity due to the low expression levels of GPCRs and the high conformational variability of extracellular epitopes on GPCRs.<sup>[18]</sup> This is especially true for the ARs that are lacking an extended extracellular N-terminus.

In the past decade, multiple small molecules have been developed as tool compounds to study the hA<sub>3</sub>AR on a molecular level. Most prominently developed are the fluorescent ligands: agonists or antagonists conjugated to a fluorophore.<sup>[19–28]</sup> Noteworthy, one of these fluorescent ligands has been used to study internalization, localization and certain PPIs of the hA<sub>3</sub>AR on hA<sub>3</sub>AR-overexpressing Chinese hamster ovary (CHO) cells, as well as activated neutrophils.<sup>[12,24]</sup> Yet, the current use of fluorescent ligands is limited to the type of fluorophore conjugated, a fluorescent read-out in specific assay types and reversible binding to the receptor. Therefore, in this study, we aimed to develop a clickable affinity-based probe (AfBP) to broaden the current possibilities to measure and detect the receptor.

AfBPs are tool compounds that consist of three parts. Firstly, an electrophilic group ('warhead') is incorporated, that ensures covalent binding of the AfBP to the receptor (Figure 1).<sup>[29,30]</sup> This allows usage of the probe in biochemical assays that rely on denaturation of proteins (e.g. SDS-PAGE and chemical proteomics). The warhead is coupled to a high affinity scaffold (the second part) that induces selectivity to the protein target of interest and thirdly, a detection moiety is introduced. Our lab has recently reported the development of electrophilic antagonist LUF7602 as an irreversible ligand of the hA<sub>3</sub>AR (Figure S1).<sup>[31]</sup> This compound contains two out of three functionalities of an AfBP, the only part missing being the detection moiety. Here, we introduced an alkyne group as ligation handle, that can be 'clicked' to a detection moiety through the Copper-catalysed Alkyne-Azide Cycloaddition (CuAAC).<sup>[32,33]</sup> Together this approach results in a 'modular' probe that can be clicked *in situ* to any detection moiety of interest. The new probe allows specific detection of overexpressed hA<sub>3</sub>AR in various assay types, such as SDS-PAGE and confocal microscopy, as well as detection of endogenous hA<sub>3</sub>AR in flow cytometry experiments on granulocytes.

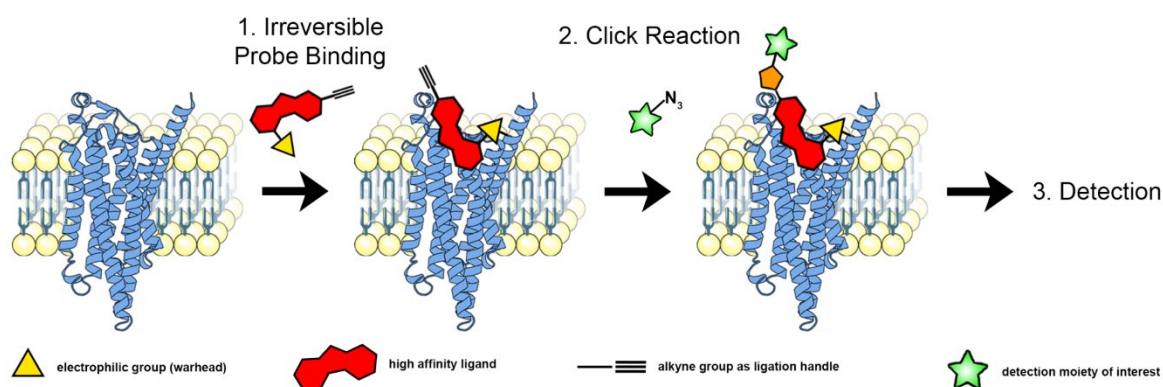


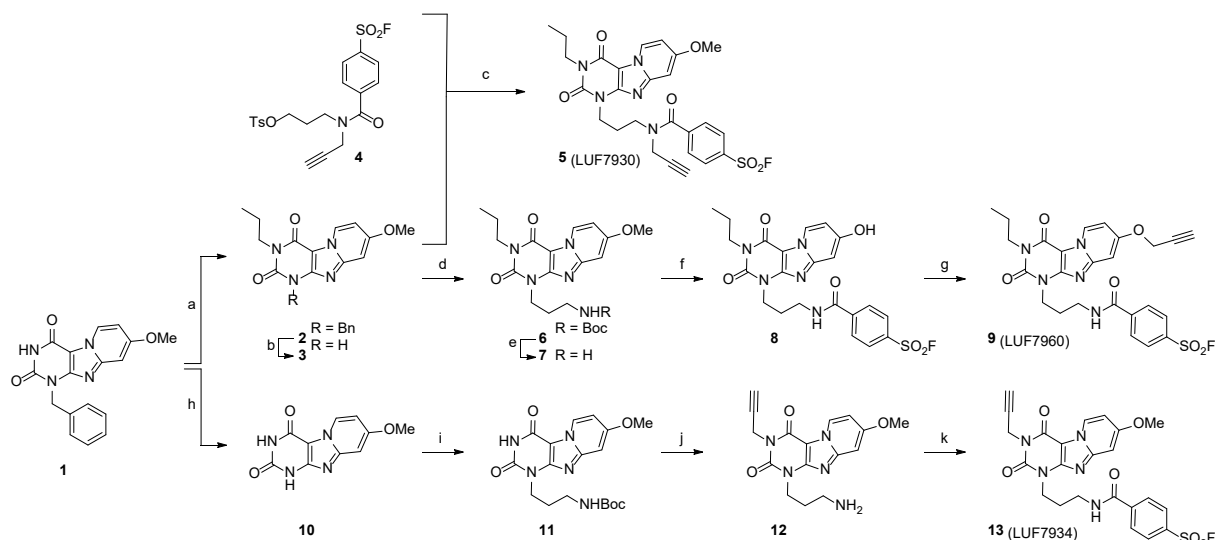
**Figure 1.** Strategy to label the hA<sub>3</sub>AR with an AfBP. First, the AfBP is added to cells or membrane fractions to allow irreversible bond formation between receptor and probe. Click reagents are then added to install a detection moiety onto the probe-bound receptor. Lastly, cells are further processed for detection, dependent on the detection method of interest. The image of the hA<sub>3</sub>AR was generated using Protein Imager,<sup>[34]</sup> using the structure of the hA<sub>3</sub>AR (AF-P0DMS8-F1) as predicted by AlphaFold.<sup>[35,36]</sup>

## Results and Discussion

### DESIGN AND SYNTHESIS

As mentioned in the introduction, a functional AfBP consists of three parts: warhead, pharmacological scaffold, and detection moiety. We decided on an alkyne moiety, to enable click-based incorporation of a detection moiety of choice onto the AfBP. Similar click strategies have already been used in the synthesis of fluorescent ligands for the hA<sub>3</sub>AR.<sup>[20,21,26,27,47]</sup> These ligands are however all lacking the electrophilic warhead. Additionally, contrary to those studies, we mainly performed the click reaction after binding of the AfBP to the receptor, preventing a loss of affinity due to bulky substituents. Such an approach has recently successfully been applied for the detection of other adenosine receptors, namely the A<sub>1</sub>AR and A<sub>2A</sub>AR.<sup>[37,48,49]</sup> Also a non-selective AfBP for the hA<sub>3</sub>AR has been reported, albeit without successful detection experiments.<sup>[48]</sup> In previous studies we observed that the position of the alkyne moiety on the scaffold can greatly influence the affinity of the AfBP towards the receptor, thereby affecting the functionality of the AfBP.<sup>[37]</sup> To increase the chances of obtaining a successful AfBP, we therefore introduced the alkyne group on three divergent locations onto the scaffold of LUF7602 (Scheme 1).

All three synthetic routes started with compound **1**, a high affinity selective antagonist for the hA<sub>3</sub>AR reported over two decades ago.<sup>[38]</sup> First, **1** was alkylated with bromopropane yielding tricyclic compound **2**. The benzylic moiety was then removed using palladium over carbon and an excess of NH<sub>4</sub>HCO<sub>2</sub>.<sup>[31]</sup> The secondary amine of **3** was alkylated with alkyne-containing fluorosulfonyl moiety **4**, synthesized as recently described,<sup>[37]</sup> to yield compound **5** (LUF7930) as the first out of three AfBPs. For the second AfBP, the secondary amine of **3** was alkylated by a protected propylamine, followed by deprotection of the Boc-group to yield compound **7**. The methoxy group of **7** was removed using BBr<sub>3</sub>, yielding a zwitterionic intermediate that, after removal of remaining BBr<sub>3</sub>, was used immediately in a peptide coupling to synthesize fluorosulfonyl derivative **8**. The alkyne moiety was then substituted onto the phenolic OH to yield compound **9** (LUF7960) as the second out of three AfBPs. For the last AfBP, the benzyl group of compound **1** was removed in the first step. However, synthesis and purification of **10** turned out to be cumbersome. Therefore a crude mixture of **10** was used in the following alkylation step, resulting in a poor but sufficient yield of compound **11**. The alkyne moiety was then substituted onto compound **11** using propargyl bromide, followed by deprotection of the Boc-group to yield compound **12**. Lastly, fluorosulfonyl benzoic acid was introduced using peptide coupling conditions, yielding compound **13** (LUF7934) as the final out of three AfBPs.



**Scheme 1** Synthesis of hA<sub>3</sub>AR-targeting affinity-based probes. Reagents and conditions: a) diazabicycloundecene (DBU), 1-bromopropane, MeCN, 70 °C, 1 h, quant.; b) Pd(OH)<sub>2</sub>/C, NH<sub>4</sub>HCO<sub>2</sub>, EtOH, 80 °C, 7 days, 53%; c) K<sub>2</sub>CO<sub>3</sub>, DMF, rt, overnight, 29%; d) *tert*-butyl (3-bromopropyl)carbamate, K<sub>2</sub>CO<sub>3</sub>, DMF, 100 °C, 2 h, 97%; e) TFA, CHCl<sub>3</sub>, 60 °C, overnight, 90%; f) (i) BBr<sub>3</sub> 1 M in DCM, CHCl<sub>3</sub>, 50 °C, 6 days; (ii) 4-fluorosulfonyl benzoic acid, EDC·HCl, DIPEA, DMF, rt, two days, 13% over two steps; g) propargyl bromide (80% in toluene), K<sub>2</sub>CO<sub>3</sub>, DMF, rt, overnight, 30%; h) Pd(OH)<sub>2</sub>/C, NH<sub>4</sub>HCO<sub>2</sub>, EtOH, 80 °C, 7 days; i) *tert*-butyl (3-bromopropyl)carbamate, K<sub>2</sub>CO<sub>3</sub>, DMF, 0-40 °C, 6 days, 25%; j) (i) propargyl bromide (80% in toluene), DBU, MeCN, rt, overnight; (ii) TFA, DCM, rt, 2 h, 67%; k) 4-fluorosulfonyl benzoic acid, EDC·HCl, DIPEA, DMF, rt, 3 h, 13%.

## AFFINITY AND SELECTIVITY TOWARDS THE hA<sub>3</sub>AR

The affinity of the synthesized AfBPs was determined in radioligand binding experiments. First, single concentration displacement assays were carried out on all four human adenosine receptors, using a final probe concentration of 1 μM (Table 1). Over 90% displacement was observed on the hA<sub>3</sub>AR, while all probes showed minimal displacement (≤25%) of radioligand on the other ARs. This indicates good selectivity towards the hA<sub>3</sub>AR over the other human ARs, a trend that was also observed in case of the parent compound.<sup>[31]</sup> Next, the ‘apparent’ affinities (depicted as pK<sub>i</sub> values) towards the hA<sub>3</sub>AR were determined using full curve displacement assays. To study the presumable covalent mode of action, the apparent affinity was determined with (pre-4h) and without (pre-0h) four hours of pre-incubation of AfBP with hA<sub>3</sub>AR, prior to addition of radioligand. The three synthesized AfBPs show very similar affinities at pre-0h with apparent pK<sub>i</sub> values in the double digit nanomolar range (Table 2). In all three cases, the apparent pK<sub>i</sub> shows a strong increase upon 4 h of pre-incubation, towards values in the single digit nanomolar range. This difference in affinity is reflected in a shift in apparent pK<sub>i</sub>. Hence, substitution of an alkyne moiety at all three of the divergent positions is well tolerated in case of binding affinity. To investigate the binding mode of the probes within the orthosteric binding pocket, covalent docking experiments were performed using the previously determined nucleophile Y265 as anchor (Figure 2).<sup>[31]</sup> All three compounds show a hydrogen bond interaction with the conserved N250 and π-π stacking with Phe168, two well-known interactions in ligand recognition in adenosine receptors.<sup>[39]</sup> Thus, the alkyne substitution seems to be well tolerated for all three of the probes, thereby supporting the outcome of the radioligand displacement experiments. To further confirm the covalent mode of action, wash-out experiments were performed. Compounds **5**, **9** and **13** all showed to bind persistently to the hA<sub>3</sub>AR, while full recovery of radioligand binding was observed in case of the reversible control compound LUF7714 (Figure 3, Figure S1).<sup>[31]</sup> Altogether, this indicates that the three synthesized AfBPs bind covalently to the hA<sub>3</sub>AR.

**Table 1.** Radioligand displacement (%) of the synthesized hA<sub>3</sub>AR probes on the four adenosine receptors.

Compound	hA <sub>1</sub> AR <sup>[a]</sup>	hA <sub>2A</sub> AR <sup>[b]</sup>	hA <sub>2B</sub> AR <sup>[c]</sup>	hA <sub>3</sub> AR <sup>[d]</sup>
----------	-----------------------------------	------------------------------------	------------------------------------	-----------------------------------

<b>5</b> (LUF7930)	2 (3, 0)	0 (0, 0)	10 (22, -2)	95 (96, 94)
<b>9</b> (LUF7960)	21 (24, 18)	7 (11, 2)	1 (0, 2)	95 (94, 96)
<b>13</b> (LUF7934)	25 (24, 26)	8 (9, 7)	5 (4, 5)	92 (90, 93)

[a] % specific [ $^3\text{H}$ ]DPCPX displacement by 1  $\mu\text{M}$  of respective probe on CHO cell membranes stably expressing the human  $\text{A}_1\text{AR}$  ( $\text{hA}_1\text{AR}$ ); [b] % specific [ $^3\text{H}$ ]ZM241385 displacement by 1  $\mu\text{M}$  of respective probe on HEK293 cell membranes stably expressing the human  $\text{A}_{2\text{A}}\text{AR}$  ( $\text{hA}_{2\text{A}}\text{AR}$ ); [c] % specific [ $^3\text{H}$ ]PSB-603 displacement by 1  $\mu\text{M}$  of respective probe on CHO-spap cell membranes stably expressing the human  $\text{A}_{2\text{B}}\text{AR}$  ( $\text{hA}_{2\text{B}}\text{AR}$ ); [d] % specific [ $^3\text{H}$ ]PSB-11 displacement at 1  $\mu\text{M}$  of respective probe on CHO cell membranes stably expressing  $\text{hA}_3\text{AR}$ . Probes were co-incubated with radioligand for 30 min at 25  $^\circ\text{C}$ . Data represent the mean of two individual experiments performed in duplicate.

**Table 2.** Time-dependent apparent affinity values of the synthesized  $\text{hA}_3\text{AR}$  probes.

Compound	$\text{pK}_i$ (pre-0h) <sup>[a]</sup>	$\text{pK}_i$ (pre-4h) <sup>[b]</sup>	Fold change <sup>[c]</sup>
<b>5</b> (LUF7930)	$7.55 \pm 0.01$	$8.52 \pm 0.05^{****}$	$9.5 \pm 1.0$
<b>9</b> (LUF7960)	$7.27 \pm 0.07$	$8.40 \pm 0.03^{****}$	$13.5 \pm 1.2$
<b>13</b> (LUF7934)	$7.17 \pm 0.04$	$8.38 \pm 0.05^{****}$	$16.6 \pm 3.5$

[a] Apparent affinity determined from displacement of specific [ $^3\text{H}$ ]PSB-11 binding on CHO cell membranes stably expressing the  $\text{hA}_3\text{AR}$  at 25  $^\circ\text{C}$  after 0.5 h of co-incubating probe and radioligand. [b] Apparent affinity determined from displacement of specific [ $^3\text{H}$ ]PSB-11 binding on CHO cell membranes stably expressing the  $\text{hA}_3\text{AR}$  at 25  $^\circ\text{C}$  after 4 h of pre-incubation with the respective probe, followed by an additional 0.5 h of co-incubation with radioligand. [c] Fold change determined by ratio  $\text{K}_i(0\text{ h})/\text{K}_i(4\text{ h})$ . Data represent the mean  $\pm$  SEM of three individual experiments performed in duplicate. \*\*\*\*  $p < 0.0001$  compared to the  $\text{pK}_i$  values obtained from the displacement assay with 0 h pre-incubation of probe, determined by a one-way ANOVA test using multiple comparisons.

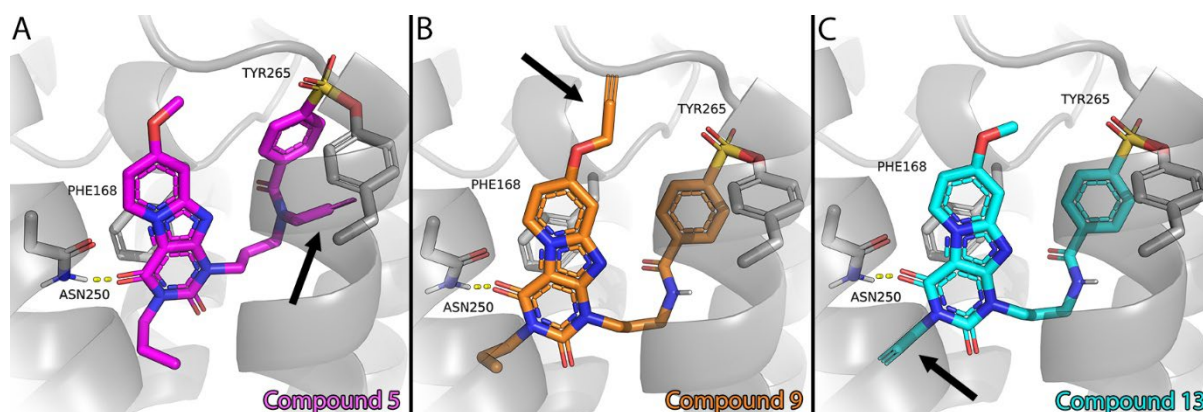


**Figure 2.** Putative binding modes of compounds 5 (panel A), 9 (panel B) and 13 (panel C). All three compounds show a hydrogen bond interaction with the conserved N250 and  $\pi$ - $\pi$  stacking with Phe168, two well-known interactions in ligand recognition in adenosine receptors.<sup>[39]</sup> The alkyne group, indicated with an arrow in each panel, fits into the binding pocket on each exit vector, and the binding orientation of the core compound, as published previously by our group, is maintained.<sup>[31]</sup>

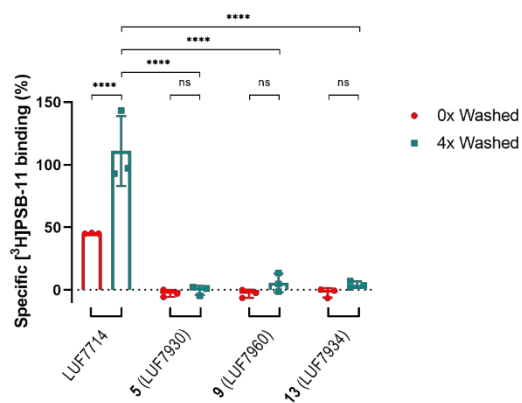


**Figure 3.** Wash-out assay reveals covalent binding of all three probes to the hA<sub>3</sub>AR. CHO cells membranes stably transfected with the hA<sub>3</sub>AR were pre-incubated with 1% DMSO (vehicle), 1 μM of non-covalent control compound (LUF7714) or 1 μM of compounds **5** (LUF7930), **9** (LUF7960) or **13** (LUF7934). The samples were washed for either 0 or 4 times, before being exposed to [<sup>3</sup>H]PSB-11 in a radioligand displacement assay. Data is expressed as the percentage of the vehicle group (100%) and represents the mean ± SEM of three individual experiments performed in duplicate. \*\*\*\* p < 0.0001 determined by a two-way ANOVA test using multiple comparisons.

## LABELING OF THE hA<sub>3</sub>AR IN SDS-PAGE EXPERIMENTS

Next, the potential AfBPs were investigated on their ability to label the hA<sub>3</sub>AR in SDS-PAGE experiments. Membrane fractions with stable expression of the hA<sub>3</sub>AR were incubated for 1 h with 50 nM (roughly the apparent K<sub>i</sub>) of AfBPs **5**, **9** or **13**, subjected to click ligation with a Cy5-fluorophore, denatured and resolved by SDS-PAGE. Pre-incubation with the hA<sub>3</sub>AR-selective antagonist PSB-11 was used as negative control,<sup>[40]</sup> and an extra incubation step with PNGase was introduced to remove N-glycans.<sup>[37]</sup> Detection of labeled hA<sub>3</sub>AR turned out to be difficult if not deglycosylated: the receptor appeared as a smear at about 70 kDa (Figure 4A and 5A). Yet, this mass corresponds to the band of rat A<sub>3</sub>AR as has been shown in SDS-PAGE experiments on overexpressing CHO cells.<sup>[41,42]</sup> N-deglycosylation of the mixture of membrane proteins revealed a protein band at ±30 kDa in case of all three AfBPs. This protein was not labeled after pre-incubation with reversible antagonist PSB-11 and is therefore most likely the hA<sub>3</sub>AR. To select one of these AfBPs for further labeling studies, the intensities of the bands at ±30 kDa were compared between the probes (Figure 4B), but no significant differences were found. Correspondingly, the alkyne groups do not inflict any strong unfavourable interactions upon covalent docking of the compounds in the hA<sub>3</sub>AR model (Figure 2). Examination of the amount of off-target labeling instead indicated there are fewer other proteins labeled by **9** (LUF7960) than by the other two probes **5** and **13** (Figure 4A). Therefore we decided to continue our subsequent experiments with AfBP **9** (LUF7960). Further control experiments were performed: labeling in CHO membrane fractions without expression of the hA<sub>3</sub>AR, no addition of probe and clicking without copper or Cy5-N<sub>3</sub> (Figure 4C). The band at ±30 kDa was not observed in any of the control lanes, confirming that this band is the hA<sub>3</sub>AR. Notably, we did not observe any hA<sub>3</sub>AR-specific labeling by a commercially available hA<sub>3</sub>AR antibody in Western Blot experiments (Figure S2). Presumably the selectivity and affinity of antibodies is compromised by the relatively short N-terminus and extracellular loops of the hA<sub>3</sub>AR.

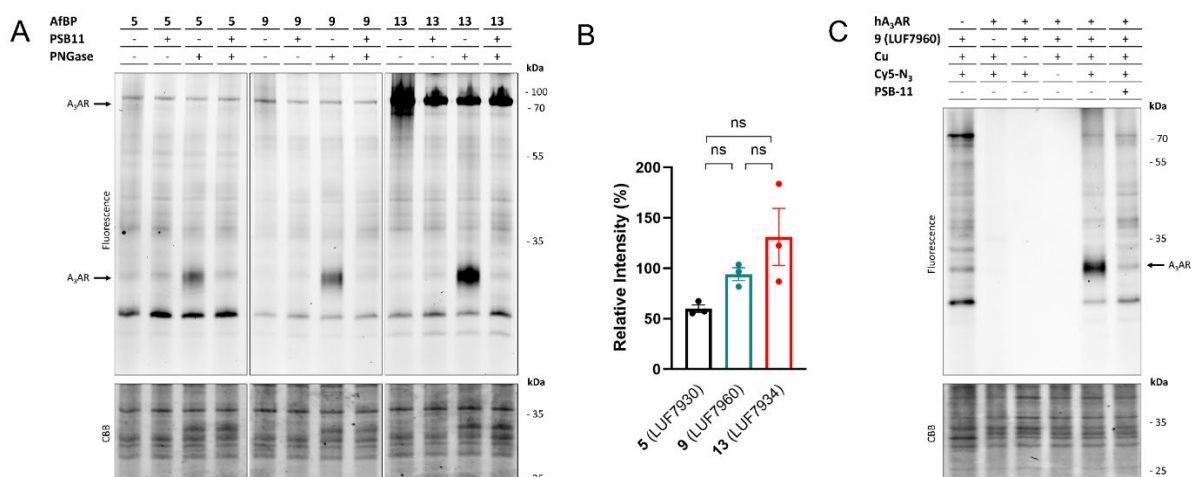


**Figure 4.** Labeling of the hA<sub>3</sub>AR by the synthesized affinity-based probes. (A) Labeling of proteins by **5** (LUF7930), **9** (LUF7960) and **13** (LUF7934). Membrane fractions from CHO cells stably overexpressing the hA<sub>3</sub>AR were pre-incubated for 30 min with antagonist (PSB-11, 1 μM final concentration) or 1% DMSO (control), prior to incubation for 1 h with the respective probe (50 nM final concentration). The proteins were subjected to PNGase or Milliq (control) for 1 h to remove N-glycans. Samples were then clicked to Cy5-N<sub>3</sub> (1 μM final concentration), denatured using Laemmli buffer (4x) and resolved by SDS-PAGE. Gels were imaged using in-gel fluorescence and stained with Coomassie Brilliant Blue (CBB) as protein loading control. (B) Quantification of the lower hA<sub>3</sub>AR band (± 30 kDa). The band intensities were taken and corrected for the observed amount of protein per lane upon CBB staining. The band at 55 kDa of the PageRuler Plus ladder (not shown) was set to 100% for each gel and band intensities were calculated relative to this band. The mean values ± SEM of three individual experiments are shown. Significance was calculated using a one-

way ANOVA test using multiple comparisons (ns = not significant), (C) Control experiments with probe **9** (LUF7960). Membrane fractions from CHO cells with or without (first lane) stable expression of the hA<sub>3</sub>AR were pre-incubated for 30 min with antagonist (PSB-11, 1 μM final concentration) or 1% DMSO (control), prior to incubation for 1 h with **9** (LUF7960) (50 nM final concentration) or 1% DMSO (control). Proteins were deglycosylated with PNGase for 1 h. Click mix was then added, containing CuSO<sub>4</sub> or MilliQ (control) and Cy5-N<sub>3</sub> (1 μM final concentration) or DMSO (control). The samples were then denatured with Laemmli buffer (4x) and resolved by SDS-PAGE. Gels were imaged using in-gel fluorescence and afterwards stained with CBB. The image shown is a representative of three individual experiments.

## LABELING OF hA<sub>3</sub>AR ON LIVE CHO CELLS

Having confirmed binding and labeling of the hA<sub>3</sub>AR in CHO membrane fractions, we moved towards labeling experiments on live CHO cells stably expressing the hA<sub>3</sub>AR. Live cells were incubated with 50 nM of AfBP **9** (LUF7960), prior to processing for either SDS-PAGE or microscopy experiments. In case of SDS-PAGE experiments, membranes were collected, the probe-bound proteins clicked to a Cy5-fluorophore, denatured and resolved by SDS-PAGE. This yielded 'cleaner' gels as compared to labeling in membrane fractions: no strong off-target bands were observed (Figure 5). The smear of glycosylated hA<sub>3</sub>AR at ±70 kDa is now better visible (Figure 5A) and absent in the control lanes (no hA<sub>3</sub>AR, no AfBP or pre-incubation with PSB-11). Similar to the experiments on cell membranes, a strong reduction in size of the band is observed upon pre-incubation with PNGase (Figure 5B). Both signals were significantly reduced by pre-incubation with PSB-11 (Figure 5C-D). Thus, AfBP **9** (LUF7960) also binds and labels the hA<sub>3</sub>AR on live cells. We speculate that the increased amount of off-target labeling in membrane fractions is due to the high enrichment of subcellular membrane proteins. Together with the electrophilic nature of the AfBP, this can result in an increased amount of protein labeling, as we have previously observed in our experiments with an electrophilic A<sub>1</sub>AR probe.<sup>[37]</sup>

In case of the microscopy experiments, cells were fixed after probe incubation, followed by a click reaction with TAMRA-N<sub>3</sub>, multiple washing steps and staining of the cellular nuclei with DAPI prior to confocal imaging. A strong increase in TAMRA intensity was observed at the cell membranes upon addition of probe to the wells (Figure 6A), visible by the increase in signal at cell-cell contacts. This signal was reduced by pre-incubation with PSB-11 and was absent for CHO cells not expressing the hA<sub>3</sub>AR (Figure 6B-C). We therefore conclude that labeling of overexpressed hA<sub>3</sub>AR by **9** (LUF7960) on living CHO cells can be studied by both SDS-PAGE and confocal microscopy experiments. Multiple fluorescent ligands have already been verified in similar fluorescence microscopy assays.<sup>[19,21–24,28]</sup> Together these fluorescent ligands comprise a molecular 'toolbox' that allows extensive characterization of the hA<sub>3</sub>AR in microscopy assays, as well as localization and internalization (with fluorescent agonists) of the receptor.<sup>[12,24]</sup> The introduction of an electrophilic warhead and clickable handle on probe **9** (LUF7960) extends the possibilities to study the hA<sub>3</sub>AR in microscopy assays, e.g. by allowing workflows that are dependent on thorough washing steps and/or denaturation of proteins.

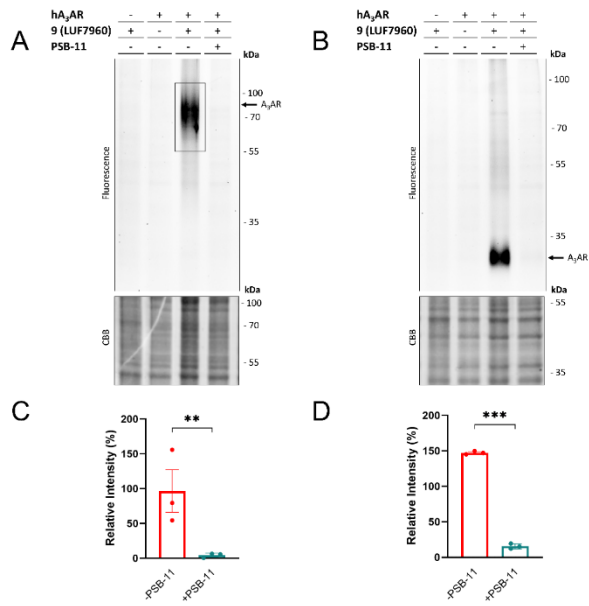


**Figure 5.** Labeling of the hA<sub>3</sub>AR on live CHO cells. CHO cells with or without (first lane) stable expression of the hA<sub>3</sub>AR were pre-incubated for 1 h with antagonist (PSB-11, 1  $\mu$ M final concentration) at 37  $^{\circ}$ C, prior to incubation with **9** (LUF7960) (50 nM final concentration) for 1 h at 37  $^{\circ}$ C. After the incubation, unbound probe was washed away with PBS. Membranes were prepared, brought to a concentration of 1  $\mu$ g/ $\mu$ L and subjected to the click reaction with Cy5-N<sub>3</sub> (1  $\mu$ M final concentration). Samples were then denatured with Laemmli buffer (4x), resolved by SDS-PAGE and imaged using in-gel fluorescence. Gels were stained by Coomassie Brilliant Blue (CBB) as loading control. (A) Labeling of deglycosylated hA<sub>3</sub>AR. PNGase was added prior to the addition of click reagents. (B) Labeling of glycosylated hA<sub>3</sub>AR. (C-D) Quantification of the observed signals with and without addition of antagonist (PSB-11). The band intensities were calculated using ImageLab and corrected for the amount of protein measured after CBB staining. The band at 55 kDa of the PageRuler Plus ladder (not shown) was set to 100% for each gel and band intensities were calculated relative to this band. The mean values  $\pm$  SEM of three individual experiments are shown. Significance was calculated by a two-way ANOVA test using multiple comparisons (\*\*\*  $p < 0.001$ ; \*\*  $p < 0.01$ ).

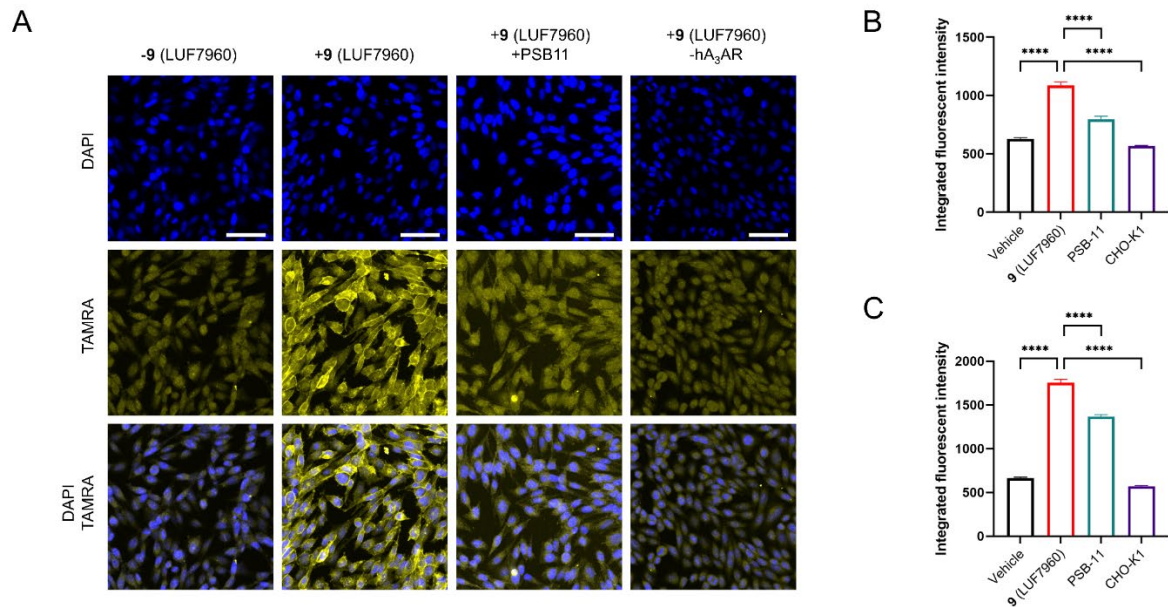


**Figure 6.** Labeling of the hA<sub>3</sub>AR observed by confocal microscopy. CHO cells with (CHO-hA<sub>3</sub>AR) or without (CHO-K1) stable expression of the hA<sub>3</sub>AR were pre-incubated for 30 min with PSB-11 (1  $\mu$ M final concentration) or 1% DMSO (control) and incubated for 60 min with **9** (LUF7960) or 1% DMSO (vehicle control). Cells were fixed, permeabilized and clicked to TAMRA-N<sub>3</sub> as fluorophore (1  $\mu$ M final concentration). The cells were then washed and kept in PBS containing 300 nM DAPI during confocal imaging. (A) Shown are DAPI staining (blue, first row), TAMRA staining (yellow, second row) and an overlay of both stains (third row). Images were acquired automatically at multiple positions in the well of interest and are representatives from two biological experiments. Scale bar = 50  $\mu$ m. Figure was created using OMERO.<sup>[43]</sup> (B-C) Comparison of the integrated fluorescence intensity between treatment conditions. Data was obtained from 2x9 fields of view, from the same experiment performed in duplicate. Each data point represents the integrated fluorescent intensity of the TAMRA signal per individual cell. Shown in the bar graphs is the average integrated fluorescence intensity of all individual cells  $\pm$  SEM. (B) N=1. (C) N=2. Significance was calculated using a one-way ANOVA test using multiple comparisons. A significant increase in intensity is observed for the cells containing the hA<sub>3</sub>AR and treated with LUF7960, versus the other conditions.

## **LABELING OF ENDOGENOUS hA<sub>3</sub>AR IN FLOW CYTOMETRY EXPERIMENTS**

Having established the potential of **9** (LUF7960) in overexpressing cell systems, we turned to native hA<sub>3</sub>AR expression in flow cytometry experiments in order to cope with expected low levels of observable fluorescence after receptor labeling caused by the notoriously low expression levels of GPCRs. Similar usage of fluorescent probes in flow cytometry experiments have thus far led to kinetic studies of ligand binding,<sup>[20,27]</sup> and detection of the hA<sub>3</sub>AR on the HL-60 model cell line.<sup>[21]</sup> In order to establish an assay setup for primary cells we first used CHO cells as a model system. To avoid the use of excess copper on live cells, AfBP **9** (LUF7960) was first clicked to a Cy5-fluorophore and desalted, before being incubated for 1 h with living CHO cells with or without stable expression of the hA<sub>3</sub>AR. Unbound probe was removed by washing steps and cells were analyzed by flow cytometry. The two types of CHO cells (+/- hA<sub>3</sub>AR) showed a difference in Cy5 mean fluorescence intensity (MFI), i.e.: hA<sub>3</sub>AR-expressing CHO cells showed a significant increase in Cy5 MFI upon probe labeling, which was absent for CHO cells without hA<sub>3</sub>AR (Figure 7A-B). Next to that, pre-incubation with PSB-11 significantly reduced the observed signal in case of the hA<sub>3</sub>AR-expressing CHO cells (Figure 7A-B), indicating that the observed signal is hA<sub>3</sub>AR-specific. Noteworthy, no significant labeling was observed with a commercially available fluorophore-conjugated hA<sub>3</sub>AR antibody.

Next we used the optimized procedure for further investigation of hA<sub>3</sub>AR expression on human granulocytes. Eosinophils and neutrophils were purified from human blood samples obtained from four donors, subjected to Cy5-clicked AfBP **9** (LUF7960) and analyzed by flow cytometry. Within these experiments, purified neutrophils did not show a significant increase in Cy5 MFI upon incubation with probe (Figure 7C). The purified eosinophils however, showed a significant increase in MFI that was reduced upon pre-incubation with the antagonist PSB-11 (Figure 7C-D). Thus, with the aid of AfBP **9** (LUF7960) we were able to selectively detect hA<sub>3</sub>AR expression on human eosinophils, but not on human neutrophils. In the past hA<sub>3</sub>AR expression has been observed on both human eosinophils and neutrophils,<sup>[7-9,12-14]</sup> though the basal hA<sub>3</sub>AR expression levels on human neutrophils were low in comparison to the expression on stimulated neutrophils.<sup>[12,13]</sup> Correspondingly, the herein investigated neutrophils showed little to no hA<sub>3</sub>AR expressed on the cell surface. Future studies that make use of AfBP **9** (LUF7960) might therefore yield new information on hA<sub>3</sub>AR expression levels on stimulated neutrophils, among other leukocytes. Furthermore, the role of the hA<sub>3</sub>AR in inflammatory conditions, such as asthma, ischemic injury and sepsis,<sup>[44-46]</sup> might be elucidated using AfBP **9** (LUF7960) as tool to detect receptor expression.

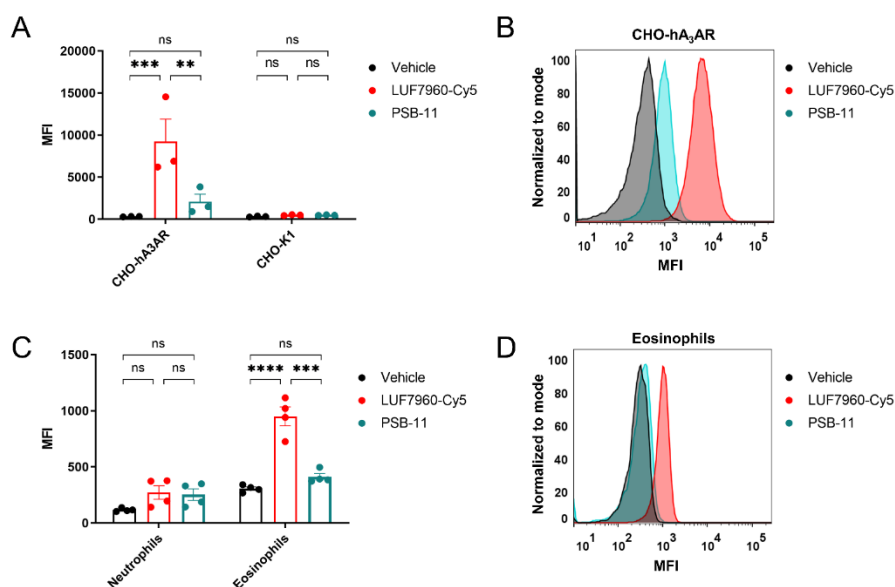


**Figure 7.** Labeling of the hA<sub>3</sub>AR in flow cytometry experiments. Samples were pre-incubated for 30 min with the antagonist PSB-11 and incubated for 60 min with **9** (LUF7960) pre-clicked to a Cy5 fluorophore (LUF7960-Cy5). Samples were then washed and analyzed on Cy5 fluorescence by flow cytometry. (A) Cy5 mean fluorescence intensity (MFI) in CHO cells with (CHO-hA<sub>3</sub>AR) and without (CHO-K1) stable expression of the hA<sub>3</sub>AR. Values represent the mean  $\pm$  SEM of three individual experiments performed in duplicate. Significance was calculated by a one-way ANOVA test using multiple comparisons (\*\*\*  $p < 0.001$ ; \*\*  $p < 0.01$ ; ns = not significant). (B) Representative graph showing the observed shift in MFI related to hA<sub>3</sub>AR labeling in CHO-hA<sub>3</sub>AR cells. (C) MFI of LUF7960-Cy5 in neutrophils and eosinophils purified from human blood samples. Values represent the mean  $\pm$  SEM (n=4) of four donors from two individual experiments. Significance was calculated by a one-way ANOVA test using multiple comparisons (\*\*\*\*  $p < 0.0001$ ; \*\*\*  $p < 0.001$ ; ns = not significant). (D) Representative graph showing the observed shift in MFI related to hA<sub>3</sub>AR labeling in human eosinophils.

## Conclusion

In this work, we have synthesized and evaluated three affinity-based probes **5**, **9** and **13**, that are all shown to bind covalently and with similar apparent affinities to the hA<sub>3</sub>AR. Although all three probes were able to label the hA<sub>3</sub>AR in SDS-PAGE experiments, we decided to continue with **9** (LUF7960) due to the low number of off-target protein bands detected on gel. We show that AfBP **9** (LUF7960) is a versatile AfBP that can be used together with different fluorophores, examples in this study being Cy5 and TAMRA. The combination of **9** (LUF7960) with click chemistry allowed us to label the hA<sub>3</sub>AR in various assay types, such as SDS-PAGE, confocal microscopy and flow cytometry experiments, on both model cell lines and cells derived from human blood samples. In our hands, **9** (LUF7960) showed to be successful in the selective labeling of the hA<sub>3</sub>AR, while commercial antibodies were not. We therefore believe that probe **9** (LUF7960) will be of great use in the detection and characterization of the hA<sub>3</sub>AR in different types of granulocytes, among other cell types.

## Acknowledgements

We thank I. Boom (LACDR, Leiden, The Netherlands) for performing high-resolution mass spectrometry measurements and B. Slütter (LACDR, Leiden, The Netherlands) for flow cytometry. We also thank the Leiden University Cell Observatory for access to the confocal microscope and support and assistance in this work.

## References

- [1] B. B. Fredholm, A. P. IJzerman, K. A. Jacobson, K.-N. Klotz, J. Linden, *Pharmacol Rev* **2001**, *53*, 527–552.
- [2] B. B. Fredholm, A. P. IJzerman, K. A. Jacobson, J. Linden, C. E. Müller, *Pharmacol Rev* **2011**, *63*, 1–34.

- [3] A. P. IJzerman, K. A. Jacobson, C. E. Müller, B. N. Cronstein, R. A. Cunha, *Pharmacol Rev* **2022**, *74*, 340–372.
- [4] L. Antonioli, P. Pacher, G. Haskó, *Trends Pharmacol Sci* **2022**, *43*, 43–55.
- [5] C. Cekic, J. Linden, *Nat Rev Immunol* **2016**, *16*, 177–192.
- [6] C. Mazziotta, J. C. Rotondo, C. Lanzillotti, G. Campione, F. Martini, M. Tognon, *Oncogene* **2022**, *41*, 301–308.
- [7] Y. Kohno, J. Xiao-Duo, S. D. Mawhrter, M. Koshiba, K. A. Jacobson, *Blood* **1996**, *88*, 3569–3574.
- [8] B. A. M Walker, M. A. Jacobson, D. A. Knight, C. A. Salvatore, T. Weir, D. Zhou, T. R. Bai, *Am J Respir Cell Mol Biol* **1997**, *16*, 531–537.
- [9] M. G. Bouma, T. M. M. A. Jeunhomme, D. L. Boyle, M. A. Dentener, N. N. Voitenok, F. A. J. M. van den Wildenberg, W. A. Buurman, *The Journal of Immunology* **1997**, *158*, 5400–5408.
- [10] J. R. Fozard, H.-J. Pfannkuche, H.-J. Schuurman, *Eur J Pharmacol* **1996**, *298*, 293–297.
- [11] D. van der Hoeven, T. C. Wan, J. A. Auchampach, *Mol Pharmacol* **2008**, *74*, 685–696.
- [12] R. Corriden, T. Self, K. Akong-Moore, V. Nizet, B. Kellam, S. J. Briddon, S. J. Hill, *EMBO Rep* **2013**, *14*, 726–732.
- [13] Y. Chen, R. Corriden, Y. Inoue, L. Yip, N. Hashiguchi, A. Zinkernagel, V. Nizet, P. A. Insel, W. G. Junger, *Science (1979)* **2006**, *314*, 1792–1795.
- [14] K. F. Alsharif, M. R. Thomas, H. M. Judge, H. Khan, L. R. Prince, I. Sabroe, V. C. Ridger, R. F. Storey, *Vascul Pharmacol* **2015**, *71*, 201–207.
- [15] K. A. Jacobson, S. Merighi, K. Varani, P. A. Borea, S. Baraldi, M. Aghazadeh Tabrizi, R. Romagnoli, P. G. Baraldi, A. Ciancetta, D. K. Tosh, Z.-G. Gao, S. Gessi, *Med Res Rev* **2018**, *38*, 1031–1072.
- [16] C. T. Leung, A. Li, J. Banerjee, Z.-G. Gao, T. Kambayashi, K. A. Jacobson, M. M. Civan, *Purinergic Signal* **2014**, *10*, 465–475.
- [17] C. K. Goth, U. E. Petäjä-Repo, M. M. Rosenkilde, *ACS Pharmacol Transl Sci* **2020**, *3*, 237–245.
- [18] M. Jo, S. T. Jung, *Exp Mol Med* **2016**, *48*, e207.
- [19] A. J. Vernall, L. A. Stoddart, S. J. Briddon, S. J. Hill, B. Kellam, *J Med Chem* **2012**, *55*, 1771–1782.
- [20] E. Kozma, T. S. Kumar, S. Federico, K. Phan, R. Balasubramanian, Z.-G. Gao, S. Paoletta, S. Moro, G. Spalluto, K. A. Jacobson, *Biochem Pharmacol* **2012**, *83*, 1552–1561.
- [21] E. Kozma, E. T. Gizewski, D. K. Tosh, L. Squarzialupi, J. A. Auchampach, K. A. Jacobson, *Biochem Pharmacol* **2013**, *85*, 1171–1181.
- [22] A. J. Vernall, L. A. Stoddart, S. J. Briddon, H. W. Ng, C. A. Laughton, S. W. Doughty, S. J. Hill, B. Kellam, *Org Biomol Chem* **2013**, *11*, 5673–5682.
- [23] L. A. Stoddart, A. J. Vernall, J. L. Denman, S. J. Briddon, B. Kellam, S. J. Hill, *Chem Biol* **2012**, *19*, 1105–1115.

- [24] L. A. Stoddart, A. J. Vernall, S. J. Briddon, B. Kellam, S. J. Hill, *Neuropharmacology* **2015**, *98*, 68–77.
- [25] S. Federico, E. Margiotta, S. Paoletta, S. Kachler, K.-N. Klotz, K. A. Jacobson, G. Pastorin, S. Moro, G. Spalluto, *Medchemcomm* **2019**, *10*, 1094–1108.
- [26] S. Federico, E. Margiotta, S. Moro, E. Kozma, Z.-G. Gao, K. A. Jacobson, G. Spalluto, *Eur J Med Chem* **2020**, *186*, 111886.
- [27] K. S. Toti, R. G. Campbell, H. Lee, V. Salmaso, R. R. Suresh, Z. G. Gao, K. A. Jacobson, *Purinergic Signal* **2022**, DOI 10.1007/s11302-022-09873-3.
- [28] M. Macchia, F. Salvetti, S. Bertini, V. di Bussolo, L. Gattuso, M. Gesi, M. Hamdan, K.-N. Klotz, T. Laragione, A. Lucacchini, F. Minutolo, S. Nencetti, C. Papi, D. Tuscano, C. Martini, *Bioorg Med Chem Lett* **2001**, *11*, 3023–3026.
- [29] D. Greenbaum, K. F. Medzihradzky, A. Burlingame, M. Bogyo, *Chem Biol* **2000**, *7*, 569–581.
- [30] Y. Liu, M. P. Patricelli, B. F. Cravatt, *Proceedings of the National Academy of Sciences* **1999**, *96*, 14694–14699.
- [31] X. Yang, J. P. D. van Veldhoven, J. Offringa, B. J. Kuiper, E. B. Lenselink, L. H. Heitman, D. van der Es, A. P. IJzerman, *J Med Chem* **2019**, *62*, 3539–3552.
- [32] V. v. Rostovtsev, L. G. Green, V. v. Fokin, K. B. Sharpless, *Angewandte Chemie - International Edition* **2002**, *41*, 2596–2599.
- [33] C. W. Tornøe, C. Christensen, M. Meldal, *Journal of Organic Chemistry* **2002**, *67*, 3057–3064.
- [34] G. Tomasello, I. Armenia, G. Molla, *Bioinformatics* **2020**, *36*, 2909–2911.
- [35] J. Jumper, R. Evans, A. Pritzel, T. Green, M. Figurnov, O. Ronneberger, K. Tunyasuvunakool, R. Bates, A. Žídek, A. Potapenko, A. Bridgland, C. Meyer, S. A. A. Kohl, A. J. Ballard, A. Cowie, B. Romera-Paredes, S. Nikolov, R. Jain, J. Adler, T. Back, S. Petersen, D. Reiman, E. Clancy, M. Zielinski, M. Steinegger, M. Pacholska, T. Berghammer, S. Bodenstein, D. Silver, O. Vinyals, A. W. Senior, K. Kavukcuoglu, P. Kohli, D. Hassabis, *Nature* **2021**, *596*, 583–589.
- [36] M. Varadi, S. Anyango, M. Deshpande, S. Nair, C. Natassia, G. Yordanova, D. Yuan, O. Stroe, G. Wood, A. Laydon, A. Žídek, T. Green, K. Tunyasuvunakool, S. Petersen, J. Jumper, E. Clancy, R. Green, A. Vora, M. Lutfi, M. Figurnov, A. Cowie, N. Hobbs, P. Kohli, G. Kleywegt, E. Birney, D. Hassabis, S. Velankar, *Nucleic Acids Res* **2022**, *50*, D439–D444.
- [37] B. L. H. Beerkens, Ç. Koç, R. Liu, B. I. Florea, S. E. le Dévédec, L. H. Heitman, A. P. IJzerman, D. van der Es, *ACS Chem Biol* **2022**, *17*, 3131–3139.
- [38] E.-M. Priego, J. von Frijtag Drabbe Kuenzel, A. P. IJzerman, M.-J. Camarasa, M.-J. Pérez-Pérez, *J Med Chem* **2002**, *45*, 3337–3344.
- [39] W. Jespers, A. C. Schiedel, L. H. Heitman, R. M. Cooke, L. Kleene, G. J. P. van Westen, D. E. Gloriam, C. E. Müller, E. Sotelo, H. Gutiérrez-de-Terán, *Trends Pharmacol Sci* **2018**, *39*, 75–89.
- [40] C. E. Müller, M. Thorand, R. Qurishi, M. Diekmann, K. A. Jacobson, W. L. Padgett, J. W. Daly, *J Med Chem* **2002**, *45*, 3440–3450.
- [41] T. M. Palmer, J. L. Benovic, G. L. Stiles, *J Biol Chem* **1995**, *270*, 29607–29613.

- [42] T. M. Palmer, G. L. Stiles, *Mol Pharmacol* **2000**, *57*, 539–545.
- [43] C. Allan, J.-M. Burel, J. Moore, C. Blackburn, M. Linkert, S. Loynton, D. MacDonald, W. J. Moore, C. Neves, A. Patterson, M. Porter, A. Tarkowska, B. Loranger, J. Avondo, I. Lagerstedt, L. Lianas, S. Leo, K. Hands, R. T. Hay, A. Patwardhan, C. Best, G. J. Kleywegt, G. Zanetti, J. R. Swedlow, *Nat Methods* **2012**, *9*, 245–253.
- [44] J. J. Reeves, C. A. Harris, B. P. Hayes, P. R. Butchers, M. J. Sheehan, *Inflammation Research* **2000**, *49*, 666–672.
- [45] L. M. Gazoni, D. M. Walters, E. B. Unger, J. Linden, I. L. Kron, V. E. Laubach, *Journal of Thoracic and Cardiovascular Surgery* **2010**, *140*, 440–446.
- [46] Y. Inoue, Y. Chen, M. I. Hirsh, L. Yip, W. G. Junger, *Shock* **2008**, *30*, 173–177.
- [47] D. K. Tosh, M. Chinn, L. S. Yoo, D. W. Kang, H. Luecke, Z.-G. Gao, K. A. Jacobson, *Bioorg Med Chem* **2010**, *18*, 508–517.
- [48] P. N. H. Trinh, D. J. W. Chong, K. Leach, S. J. Hill, J. D. A. Tyndall, L. T. May, A. J. Vernall, K. J. Gregory, *J Med Chem* **2021**, *64*, 8161–8178.
- [49] X. Yang, T. J. M. Michiels, C. de Jong, M. Soethoudt, N. Dekker, E. Gordon, M. van der Stelt, L. H. Heitman, D. van der Es, A. P. IJzerman, *J Med Chem* **2018**, *61*, 7892–7901.